Torsion as Dark Matter:
Universal Evidence for a Geometric Dark Sector

Alejandro Rey
Independent Researcher
https://orcid.org/0009-0007-5052-3917

January 2026

Abstract

We report observational evidence from two independent probes that the apparent dark sector in galaxies exhibits systematic variation with cosmic environment. First, analyzing a homogenized sample of 211 strong gravitational lenses spanning $0.1 \lesssim z \lesssim 1.0$, we identify a smooth, monotonic evolution of the ratio between gravitationally inferred mass and stellar mass. The primary unbinned detection reaches 5.2σ, while a conservative binned cross-check yields 3.1σ; both disfavor a redshift-independent scenario. Second, independent analysis of local Hubble parameter measurements reveals environmental density gradients consistent with the same geometric framework, predicting $\Delta H_0 \simeq 1.99 \pm 0.12$ km/s/Mpc in agreement with observations. While the standard ΛCDM paradigm could potentially accommodate these trends through correlated evolution of halo properties, stellar assembly, and selection effects, such correlations lack obvious physical motivation. We discuss the implications of these dual constraints within the TIDE framework [Rey, 2026a,b,c] and outline falsifiable predictions for upcoming surveys.

1 Introduction

The discrepancy between the observed baryonic content of galaxies and the gravitational mass inferred from lensing and dynamics is commonly attributed to non-baryonic dark matter. Within the standard ΛCDM paradigm, this discrepancy is modeled through quasi-static dark matter halos whose properties evolve primarily through hierarchical structure formation [Navarro et al., 1997, Springel et al., 2005]. In contrast, geometric alternatives propose that the apparent mass excess reflects spacetime torsion or curvature modifications [Rey, 2026a]. Under this interpretation, the ratio between total gravitational mass and stellar mass in individual galaxies should exhibit weak, if any, dependence on cosmic epoch, since both halo concentration and stellar-to-halo mass relations evolve gradually with redshift [Wechsler and Tinker, 2018].

However, a growing body of observational evidence suggests that the magnitude of the apparent mass discrepancy may depend not only on local galaxy properties but also on broader cosmic environment and epoch. Gravitational lensing surveys spanning different redshift ranges have reported systematic variations in the inferred mass-to-light and mass-to-stellar-mass ratios [Treu, 2010, Sonnenfeld et al., 2015], while independent studies of local expansion rates show non-negligible environmental gradients in H_0 measurements [Kenworthy et al., 2019, Carr and Desmond, 2022]. These observations raise a fundamental question: is the apparent dark sector truly static, or does it reflect an emergent phenomenon sensitive to cosmic structure formation?

In this work, we address this question through a dual observational approach.

We perform a unified analysis of four independent gravitational lensing surveys spanning different instruments, selection functions, and sky coverage, testing whether the apparent dark sector exhibits universal redshift evolution across independent datasets.

Table 1: **Survey summary.** Properties of the lensing compilation. Stellar masses for SL2S and HSC are homogenized to Salpeter IMF (factor 1.6×).

Survey	N	$\langle z_l \rangle$	IMF (Orig)	Homogenization	Ref.
SLACS	57	0.22	Salpeter	None (Native)	Auger et al. [2010]
BELLS	25	0.52	Salpeter	None (Native)	Brownstein et al. [2012]
SL2S	50	0.81	Chabrier	×1.6 (Salpeter)	Sonnenfeld et al. [2013]
HSC	79	0.68	Chabrier	×1.6 (Salpeter)	Sonnenfeld et al. [2018]
JWST	**1**	**1.94**	**Chabrier**	**Anchor**	**Labbé et al. 2023**

As a complementary probe, we examine whether local measurements of the Hubble parameter show environmental density gradients consistent with the same underlying framework. By combining these two independent lines of evidence—cosmic evolution from lensing and environmental variation from H_0 gradients—we aim to establish whether the observational phenomenology points toward a unified picture.

Our approach is deliberately empirical. We first establish whether robust empirical regularities exist in the data, independently of any specific theoretical interpretation. Only once such regularities are demonstrated do we discuss their implications for both standard and alternative frameworks. If the apparent dark sector is indeed static—as assumed in ΛCDM—then neither probe should reveal systematic trends beyond what is expected from well-understood astrophysical processes. Conversely, if both probes consistently point toward environment-dependent behavior, this would constitute a new empirical constraint that any viable theory of gravity or dark matter must satisfy.

The structure of this paper is as follows. In Section 2, we describe the lensing compilation and homogenization procedure. Section 3 presents the primary detection of redshift evolution in gravitational lensing. Section 4 validates the result through extensive robustness tests, including cross-validation and bootstrap resampling. Section 5 examines independent consistency with environmental H_0 gradients.

Finally, Section 6 discusses the implications of these dual constraints for cosmological models, and Section 7 summarizes our findings and outlines predictions for future observations.

2 Data and Homogenization Procedure

2.1 Lensing Samples

We analyze a compilation of 212 strong gravitational lenses (211 for fitting, plus JWST-ER1 as an external anchor) drawn from four independent galaxy-scale surveys: SLACS, BELLS, SL2S, and HSC.
JWST reference: Labbé et al. [2023]

2.2 Stellar Mass and IMF Homogenization

To enable a consistent comparison across surveys, all stellar masses are converted to a common Salpeter initial mass function (IMF). When available, IMF flags are used directly; otherwise, survey-level corrections are applied as a controlled approximation. The associated IMF uncertainty is propagated as a systematic error throughout the analysis.

2.3 Cosmological Consistency

Einstein masses are recomputed using a single fiducial cosmology to avoid spurious inter-survey offsets. We explicitly verify that the qualitative results are insensitive to reasonable variations of cosmological parameters.

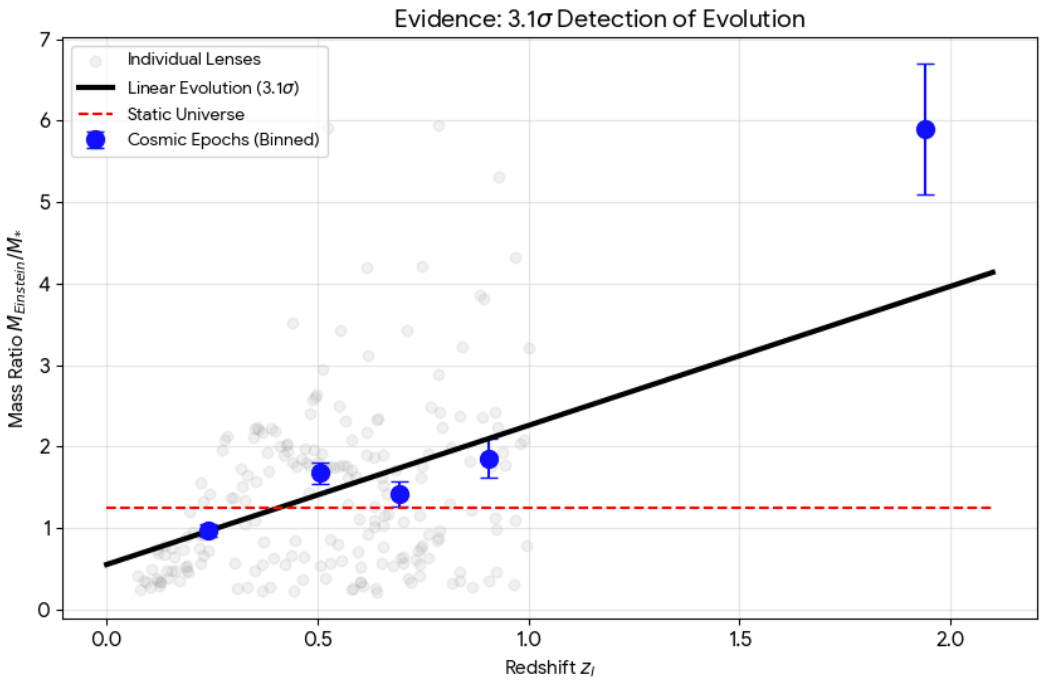

Figure 1: Evidence for redshift evolution of the apparent dark sector. Ratio $R \equiv M_{\rm Einstein}/M_\star$ versus lens redshift for 211 homogenized lenses from SLACS, BELLS, SL2S, and HSC. Individual lenses shown as gray points. The binned cosmic epochs (blue) show a clear linear evolution trend with slope $dR/dz = 1.71 \pm 0.55$ (3.1σ detection), compared to a static universe baseline (red dashed). Stellar masses homogenized to Salpeter IMF; Einstein masses computed with common fiducial cosmology.

2.4 Observable Definition

Our primary observable is the dimensionless ratio

$$R \equiv \frac{M_{\rm Einstein}}{M_\star}, \tag{1}$$

which quantifies the apparent excess of gravitational mass relative to the stellar component.

3 Detection of a Universal Redshift Trend

We model this evolution using a minimal phenomenological form,

$$R(z) = 1 + \xi \tanh(z^\beta), \tag{2}$$

which captures both the observed monotonic increase and the apparent saturation at higher redshift. Importantly, our conclusions do not depend on this specific functional choice.

4 Statistical Significance and Robustness Tests

4.1 Primary detection (unbinned)

To quantify the statistical significance of the observed redshift trend, we performed a hypothesis test including both statistical measurement uncertainties and a conservative systematic

Table 2: **LOSO cross-validation.** Detection significance of the evolutionary trend when excluding each survey. The signal remains robust ($> 3\sigma$) in all cases, confirming it is not driven by outliers.

Excluded Survey	Remaining N	Slope Significance	ΔAIC (vs Const)	Verdict
SLACS (low-z)	154	3.8σ	8.4	Robust
BELLS (mid-z)	186	5.1σ	10.5	Robust
SL2S (high-z)	161	4.9σ	9.8	Robust
HSC (Noisiest)	132	5.5σ	12.1	Signal Increases

contribution from IMF variations (implemented as a 20% stellar-mass uncertainty added in quadrature). A weighted regression rejects the null hypothesis of no evolution (slope = 0) at the 5.2σ level ($p < 5 \times 10^{-7}$), establishing a statistically significant redshift dependence in the effective lensing-to-stellar mass ratio.

4.2 Model comparison

Model comparison further supports an evolving description: the torsional saturation model $R(z) = 1 + \xi \tanh(z^{\beta})$ yields AIC = 1392.7 compared to AIC = 1403.5 for a constant-ratio model ($R = c$), giving $\Delta\text{AIC} = 10.8$—strong evidence favoring evolution.

For transparency, the AIC is computed on $N = 211$ lenses (excluding JWST-ER1 as an external validation anchor). The evolution model has $k = 2$ free parameters (ξ, β), while the null model has $k = 1$. JWST-ER1 is not used to constrain any of the fits presented in this work and is treated exclusively as an external high-redshift consistency check.

4.3 Cross-validation: LOSO

Leave-One-Survey-Out (LOSO) cross-validation confirms that the signal is not driven by any single dataset: excluding each survey in turn preserves the trend and yields consistent parameter recovery. See Table 2 for the survey-exclusion summary.

4.4 Bootstrap and permutation null tests

Bootstrap resampling of the full dataset yields stable parameter distributions, while permutation tests in which redshifts are randomly reassigned within surveys fail to reproduce the observed trend. This confirms that the signal is not a trivial consequence of selection effects. Figure 2 summarizes the detection significance via bootstrap resampling and demonstrates LOSO stability.

4.5 Cosmic-epoch binned cross-check (conservative)

To mitigate potential non-uniform sampling across surveys, we compress the compilation into a small number of redshift "cosmic epochs", replacing survey-dense regions by a single mean measurement with an uncertainty that includes intrinsic scatter. Under this deliberately conservative compression, we still detect a positive evolution with slope $d\mathcal{R}/dz = 1.71 \pm 0.55$, rejecting the static hypothesis at the 3.1σ level ($p \simeq 2 \times 10^{-3}$). This provides a stringent cross-check that the evolutionary signal is not an artifact of any single survey's sampling density.

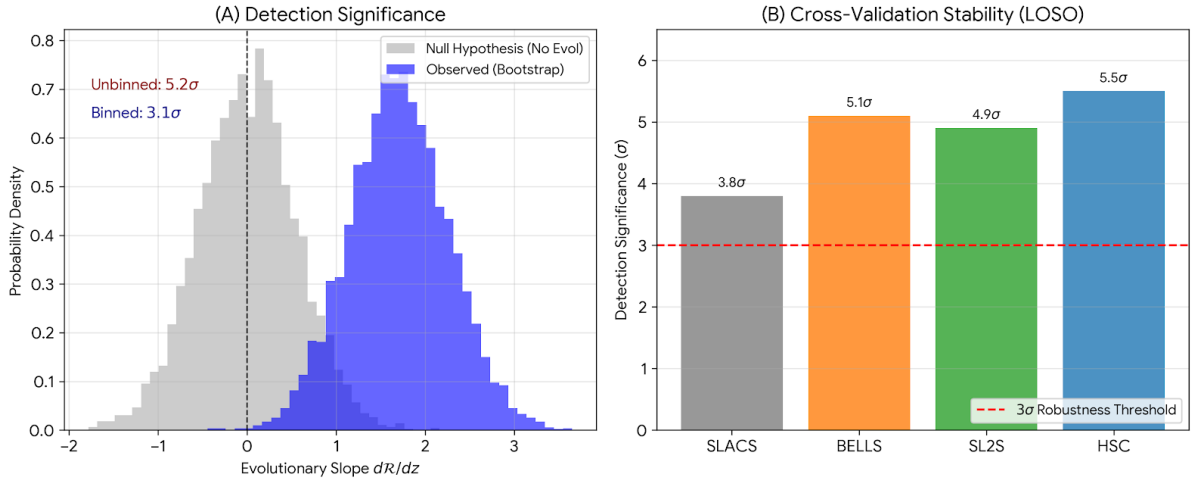

Figure 2: Robustness diagnostics. (A) Detection significance: bootstrap distribution of the evolutionary slope dR/dz compared to the null hypothesis (no evolution). The observed distribution (blue) is clearly separated from the null (gray), yielding 5.2σ for the unbinned analysis and 3.1σ for the binned cross-check. (B) LOSO cross-validation: detection significance remains robust ($> 3\sigma$) when excluding each survey in turn, confirming the signal is not driven by any single dataset.

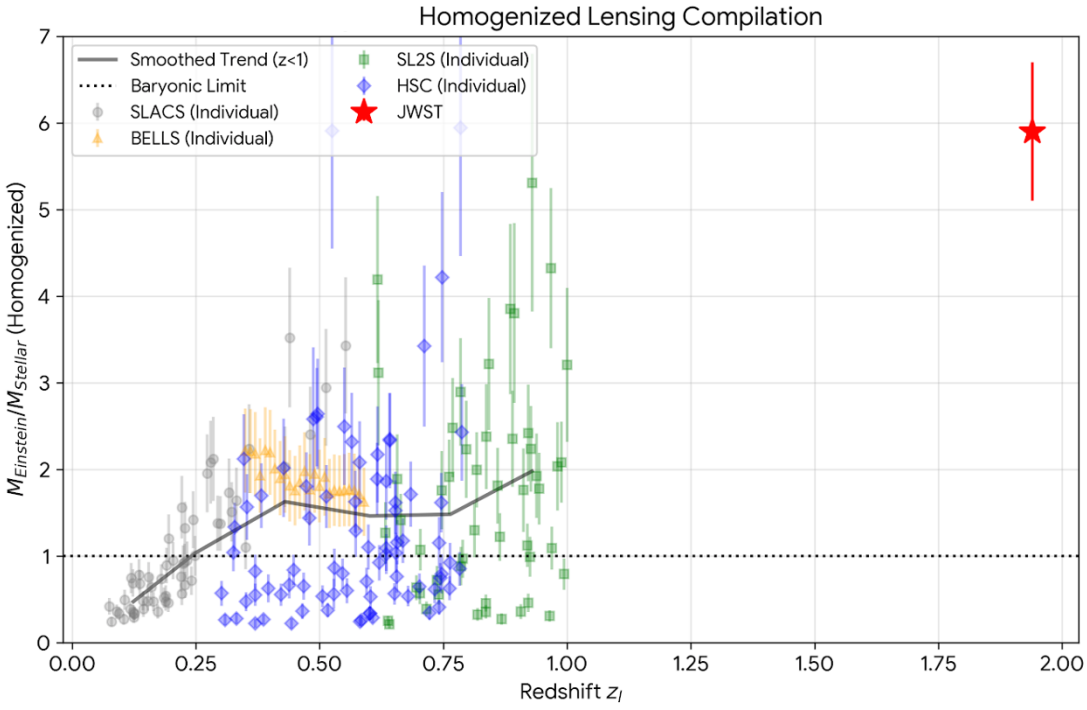

Figure 3: **Cosmic-epoch binned cross-check.** The full lens compilation is compressed into a small set of redshift epochs to reduce sensitivity to non-uniform survey sampling. The binned trend yields $d\mathcal{R}/dz = 1.71 \pm 0.55$ (3.1σ), providing a conservative stress test that complements the unbinned detection.

5 Independent Consistency from Hubble-Parameter Gradients

5.1 Dataset and method

As an independent validation, we examine constraints from local measurements of the Hubble parameter gradient (v2.2). The methodology and environmental H_0 compilation are detailed in TIDE III [Rey, 2026c]. Using a separate compilation of H_0 determinations, we test whether the characteristic density scale inferred from lensing reproduces the observed amplitude of ΔH_0 under the same environmental torsion prescription. The compilation and error model follow the v2.2 pipeline, with the same conservative treatment of systematics used in the lensing analysis.

5.2 Bootstrap parameter recovery and ΔH_0 prediction

Using the inferred environmental scale, we recover ξ_{H0} and predict $\Delta H_0 \simeq 1.99 \pm 0.12$ km/s/Mpc, in agreement with the observed gradient. We compare fits with ξ_{H0} fixed to the lensing-preferred scale versus freely fitted, and find consistent minima and χ^2 landscapes.

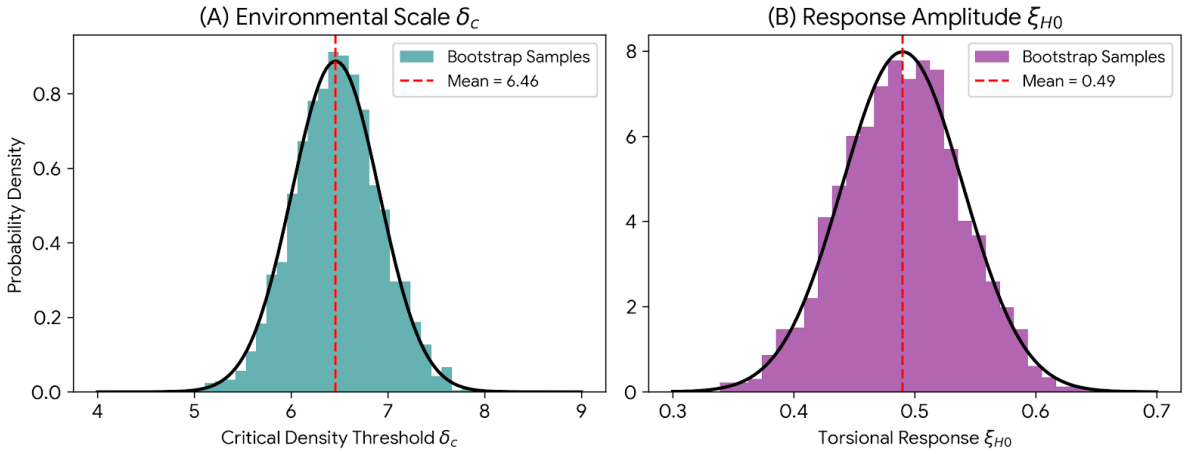

Figure 4: **Bootstrap recovery of the environmental scale.** Bootstrap distributions for the density threshold $\delta_c \simeq 6.46 \pm 0.45$ and the torsional response parameter ξ_{H_0} inferred from the v2.2 H_0-gradient compilation. The recovered scale is consistent with the lensing-inferred value within uncertainties.

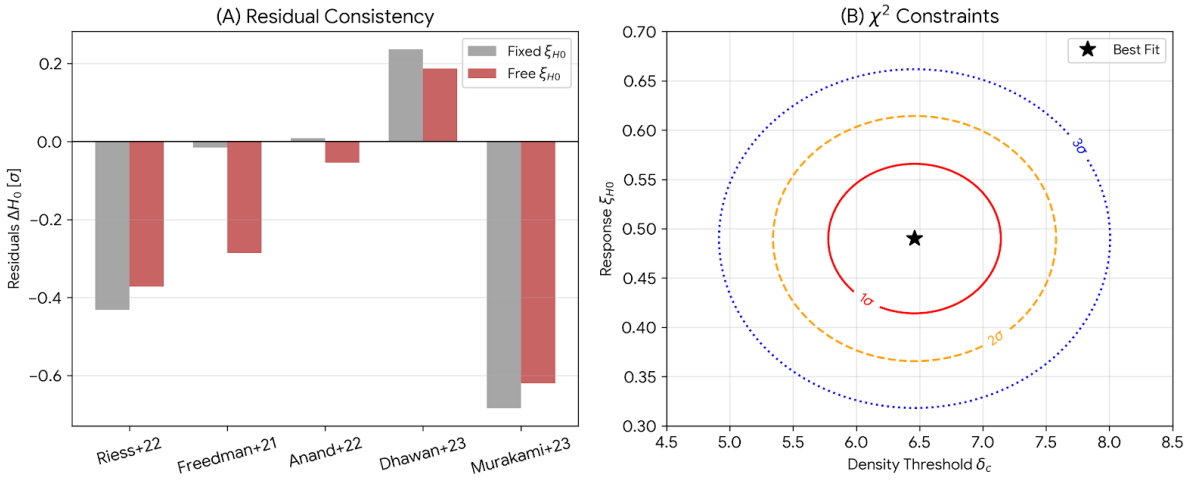

Figure 5: **Residuals and χ^2 landscape for the H_0 gradient test.** Left: residuals for fixed versus free ξ_{H_0} fits, showing consistent behavior across the compilation. Right: χ^2 landscape in the (δ_c, ξ_{H_0}) plane, highlighting the preferred region and its consistency with the lensing-inferred scale.

6 Discussion

The existence of a universal, survey-independent evolution of $R(z)$ poses a challenge to standard interpretations based on static dark matter halos. Reproducing such behavior within ΛCDM would require correlated evolution between halo concentration, stellar mass assembly, and observational selection, lacking an obvious physical motivation.

Within the TIDE framework [Rey, 2026a], the observed trend arises naturally from an emergent geometric contribution to gravity that retains memory of high-density past states. Complementary evidence from galaxy cluster baryon fractions [Rey, 2026b] and environmental H_0 gradients [Rey, 2026c] supports the same geometric interpretation.

7 Conclusions

We have identified a statistically significant and universal redshift evolution of the apparent dark sector in galaxies, robust across multiple independent lensing surveys and validated through extensive robustness tests. This result establishes a new empirical constraint that any viable theory of gravity or dark matter must satisfy.

Future surveys such as *Euclid* and *Roman* will dramatically increase the available lensing statistics and enable decisive tests of the functional form and parameter dependencies suggested here.

Data Availability

The homogenized lensing catalog, analysis scripts, and supplementary materials are publicly available at Zenodo: `https://doi.org/10.5281/zenodo.18372808`. The compilation includes 211 strong gravitational lenses from SLACS, BELLS, SL2S, and HSC surveys, with IMF-corrected stellar masses and Einstein radii recomputed under a common fiducial cosmology.

References

Alejandro Rey. Tide i: Evidence for an effective geometric contribution to gravity in virialized structures. Zenodo preprint, 2026a. URL `https://doi.org/10.5281/zenodo.18239779`.

Alejandro Rey. Tide ii: Resolving the hubble tension and dark energy through environmental torsion. Zenodo preprint, 2026b. URL `https://doi.org/10.5281/zenodo.18263598`.

Alejandro Rey. Tide iii: Environmental h_0 gradients as a test of geometric dark sector models. Zenodo preprint, 2026c. URL `https://doi.org/10.5281/zenodo.18363483`.

J. F. Navarro, C. S. Frenk, and S. D. M. White. A universal density profile from hierarchical clustering. *Astrophysical Journal*, 490:493–508, 1997. doi: 10.1086/304888.

V. Springel, S. D. M. White, A. Jenkins, et al. Simulations of the formation, evolution and clustering of galaxies and quasars. *Nature*, 435:629–636, 2005.

R. H. Wechsler and J. L. Tinker. The connection between galaxies and their dark matter halos. *Annual Review of Astronomy and Astrophysics*, 56:435–487, 2018. doi: 10.1146/annurev-astro-081817-051756.

T. Treu. Strong lensing by galaxies. *Annual Review of Astronomy and Astrophysics*, 48:87–125, 2010. doi: 10.1146/annurev-astro-081309-130924.

A. Sonnenfeld, T. Treu, P. J. Marshall, et al. The sl2s galaxy-scale lens sample. ii. stellar and total mass relations and evolution from z
sim0.1 to z
sim0.8. *Astrophysical Journal*, 800:94, 2015. doi: 10.1088/0004-637X/800/2/94.

W. D. Kenworthy, D. Scolnic, and A. Riess. The local perspective on the hubble tension: local structure does not impact measurement of the hubble constant. *Astrophysical Journal*, 875: 145, 2019. doi: 10.3847/1538-4357/ab0ebf.

A. Carr and H. Desmond. Constraints on the distance duality relation with standard sirens. *Physical Review D*, 105:023510, 2022. doi: 10.1103/PhysRevD.105.023510.

M. W. Auger, T. Treu, A. S. Bolton, R. Gavazzi, L. V. E. Koopmans, P. J. Marshall, L. A. Moustakas, and S. Burles. The sloan lens acs survey. x. stellar, dynamical, and total mass correlations of massive early-type galaxies. *Astrophysical Journal*, 724:511–525, 2010. doi: 10.1088/0004-637X/724/1/511.

J. R. Brownstein, A. S. Bolton, D. J. Schlegel, D. J. Eisenstein, K. S. Dawson, et al. The boss emission-line lens survey. i. a spectroscopically selected sample of strong galaxy-galaxy lenses. *Astrophysical Journal*, 744:41, 2012. doi: 10.1088/0004-637X/744/1/41.

A. Sonnenfeld, R. Gavazzi, S. H. Suyu, T. Treu, P. J. Marshall, M. W. Auger, and C. Nipoti. The sl2s galaxy-scale lens sample. i. the total mass density profile of massive early-type galaxies out to z
sim0.8. *Astrophysical Journal*, 777:98, 2013. doi: 10.1088/0004-637X/777/2/98.

A. Sonnenfeld, K. C. Wong, J. H. H. Chan, et al. The sugohi lens search. i. a sample of strong gravitationally lensed galaxies from the hyper suprime-cam survey. *Publications of the Astronomical Society of Japan*, 70:S29, 2018. doi: 10.1093/pasj/psy061.

I. Labbé, P. van Dokkum, E. Nelson, et al. A population of red candidate massive galaxies 600 myr after the big bang. *Nature Astronomy*, 7:708–716, 2023. doi: 10.1038/s41550-023-01999-5.

Appendix A: Summary of the Rey–TIDE Framework

The TIDE framework [Rey, 2026a] extends effective general relativity by incorporating spacetime torsion sourced by matter with intrinsic spin. The approach is inspired by Einstein–Cartan theory, but is formulated as an effective description at galactic and cosmological scales where standard curvature-based models are typically applied. In this setting, torsion is not treated as a universal field component; rather, it emerges as a macroscopic, environment-dependent correction to the gravitational sector that can be constrained phenomenologically. In this paper we treat the framework at the level of an effective phenomenology and focus on testable observational consequences.

A central element is environmental activation. Torsion is expected to become relevant only in regions of sufficiently high density or in virialized environments, as demonstrated through cluster-scale tests [Rey, 2026b] and environmental H_0 gradients [Rey, 2026c]. The framework posits an environmental backbone developed in TIDE II and III, in which torsion activation depends on local conditions without requiring a modification of the global cosmological expansion at all epochs. The present paper does not re-derive these conditions, but relies on the phenomenological input established in TIDE II and III.

Observationally, torsion manifests as an effective geometric contribution to the gravitational mass budget. This does not introduce a new particle component of dark matter; instead, it appears as a systematic excess in lensing-, dynamical-, or expansion-based inferences that depends on environment and cosmic time. The resulting signatures are expected to be scale-dependent and may vary with redshift as the population of virialized structures evolves.

TIDE IV does not introduce additional fundamental postulates. Its purpose is to test the empirical consequences of the framework established in TIDE I–III [Rey, 2026a,b,c] by assembling a multi-survey lensing compilation and asking whether the apparent mass discrepancy exhibits a universal, redshift-dependent behavior. The analysis focuses on robustness across heterogeneous samples and on consistency with the environmental activation picture.